Pseudovertical Temperature Profiles in a Broad Valley from Lines of Temperature Sensors on Sidewalls

C. DAVID WHITEMAN AND SEBASTIAN W. HOCH

University of Utah, Salt Lake City, Utah

(Manuscript received 14 July 2014, in final form 21 September 2014)

ABSTRACT

Pseudovertical temperature ''soundings'' from lines of inexpensive temperature sensors on the sidewalls of Utah's Salt Lake valley are compared with contemporaneous radiosonde soundings from the north, open end of the valley. Morning [0415 mountain standard time (MST)] soundings are colder, and afternoon (1615 MST) soundings are warmer than radiosonde soundings because of warm and cold boundary layers that form over the slopes. Cross-valley temperature differences occur between east- and west-facing sidewalls because of differing insolation. Differences in vertically averaged pseudovertical and radiosonde temperatures are generally within 1°C, with a standard deviation of 2°–3°C. The pseudovertical soundings are especially good proxies for radiosondes in winter. The sounding comparisons identified along-valley differences in temperature, inversion depth, and lapse rate that have led to hypotheses concerning their causes, to be evaluated with future research. The low cost and much better time resolution of the pseudovertical soundings suggest that such lines will be a useful supplement to valley radiosondes and will have significant operational advantages if available in real time. Lines of surface-based sensors will prove useful in identifying intravalley meteorological differences and may be used to estimate free-air temperature structure in other valleys where radiosondes are unavailable.

1. Introduction

Studies of the temporal evolution of the boundary layer structure are often limited by the high costs and low temporal resolution of radiosonde or tethersonde data. This research note addresses the feasibility of using "pseudovertical temperature" (PVT) data from inexpensive temperature sensors deployed along valley sidewalls as proxies for free-air temperature soundings. Such data would be valuable for urban planning, ecosystem monitoring, fire behavior investigations, air pollution studies, weather forecasting, and other applications.

A recent study investigated the conditions under which PVT soundings from three lines of surface stations on the sidewalls of a small closed basin would provide useful proxies for free-air tethersonde soundings over the basin center (Whiteman et al. 2004; Steinacker et al. 2007) on two June days. For stable nighttime conditions with low background winds, the PVT soundings were good proxies for free-air temperature soundings, with a mean nighttime temperature bias of 0.4°C and a standard deviation of 0.4°C. On a windy night, standard deviations increased to 1°–2°C. After sunrise the PVT soundings became less useful because of solar-driven microclimatic differences among the surface stations. In this paper we expand on this research to compare PVT and free-air temperature soundings in a broad, deep valley.

2. The Salt Lake valley and the instrumentation

Utah's Salt Lake valley (Fig. 1) is an urbanized north–south-oriented valley that drains into the Great Salt Lake. The Wasatch Mountains, with a ridgeline elevation of about 3500 m MSL, border the valley on the east; the Oquirrh Mountains, with ridgeline elevations of about 3000 m MSL, border the valley to the west. The ridge-to-ridge distance across the valley is approximately 50 km, with a valley floor width of about 20 km. The valley is open to the north and northwest where the Jordan River flows into the Great Salt Lake. Its drainage area extends far southward into the Utah Lake valley, but a transverse mountain range 30 km south of Salt

Corresponding author address: C. David Whiteman, University of Utah, Department of Atmospheric Sciences, 135 S 1460 E Rm. 819, Salt Lake City, UT 84112-0110.
E-mail: dave.whiteman@utah.edu

DOI: 10.1175/JAMC-D-14-0177.1

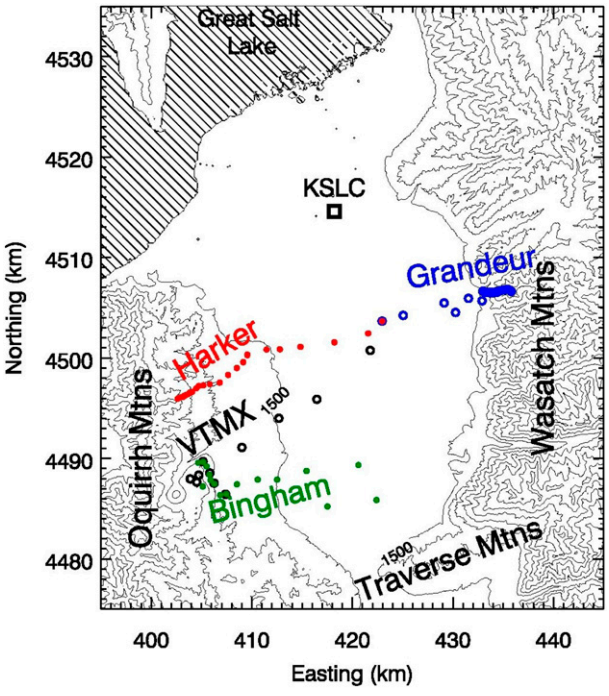

FIG. 1. Universal transverse Mercator zone-12 topographic map of the Salt Lake valley showing the radiosonde launch site (KSLC) and the Harker ridge, Grandeur ridge, Bingham, and VTMX lines of temperature dataloggers (dots). The contour interval is 250 m.

Lake City tends to give the northern segment of the Jordan River valley, the Salt Lake valley, a basinlike character.

In this paper we compare PVT soundings from lines of temperature sensors on the valley sidewalls with contemporaneous radiosondes launched from the valley floor at the Salt Lake City International Airport (KSLC; 40.7781°N, 111.9694°W; 1288 m MSL) at approximately 0415 and 1615 mountain standard time (MST; nominally, the 1200 and 0000 UTC soundings). These launch times are quite close to the times of diurnal temperature minima and maxima. The 0415 MST sounding is before astronomical sunrise and the 1615 MST sounding is before astronomical sunset throughout the entire year. Radiosonde temperature accuracies in the encoded Global Telecommunication System soundings are about 1°C (Office of the Federal Coordinator for Meteorological Services and Supporting Research 1997).

Lines of self-contained, battery-operated temperature dataloggers (HOBO Pro Temperature/External Temperature dataloggers, versions 1 and 2; Onset Computer Corporation, Bourne, Massachusetts) were deployed on the valley sidewalls in connection with two major meteorological field experiments: the Vertical Transport and Mixing Experiment (VTMX; Doran et al. 2002) and Persistent Cold-Air Pool Study (PCAPS; Lareau et al. 2013). Both campaigns had extensive deployments of surface stations reporting in real time at 5–15-min intervals. The datalogger lines were particularly valuable because they used identical sensors sited in a similar fashion and extended to elevations not covered by the routine surface network.

In the VTMX experiment the temperature dataloggers were placed on a single line running from the valley floor up the southwest sidewall (Fig. 1) and were operated between January 2000 and September 2001. In the PCAPS experiment the Grandeur ridge, Harker ridge, and Bingham lines ran up the east, west, and southwest sidewalls (Fig. 1) and were operated during the 2010/11 winter season. The HOBO elevation accuracy was about ±10 m in both experiments.

HOBOs have been previously tested in the laboratory and the field (Whiteman et al. 2000) and HOBOs and similar dataloggers have been used extensively in other meteorological projects (e.g., Clements et al. 2003; Mayr et al. 2004; Lundquist and Cayan 2007; Lundquist et al. 2008; Whiteman et al. 2008, 2010; Zawar-Reza et al. 2013). Individual HOBOs were sited to avoid nonrepresentative microclimates and obtain the best comparisons to free-air soundings. Loggers were secured on steel fence posts on the crests of ridges that ran down the sidewalls, with thermistor temperature sensors exposed in six-plate naturally aspirated radiation shields (Model 41303; R. M. Young Company, Traverse City, Michigan) at heights of 1.3 m AGL. The temperature sensors had a 2-min time constant, and temperatures were sampled and stored at 5-min intervals. HOBO temperature accuracy is ±0.4°C over the range from −10° to 50°C. Sensors in naturally aspirated radiation shields have an additional uncertainty associated with overheating of the radiation shields when winds are weak and radiation is strong. According to the manufacturer, this additional error for solar radiation of 1080 W m^{-2} varies from 0.4°C in a 3 m s^{-1} wind to 1.5°C in a 1 m s^{-1} wind.

3. Analysis results

a. Entire dataset, PCAPS and VTMX lines

HOBO–radiosonde temperature differences were obtained by averaging HOBO temperatures over the 15 min following the approximate radiosonde launch time and subtracting from this the radiosonde temperature interpolated to the nearest whole 10-m height interval. Periods of record for the HOBO data for the two experiments are shown in Fig. 2. Temperature differences, standard deviations and numbers of observations are shown in Fig. 3 for the entire period of record.

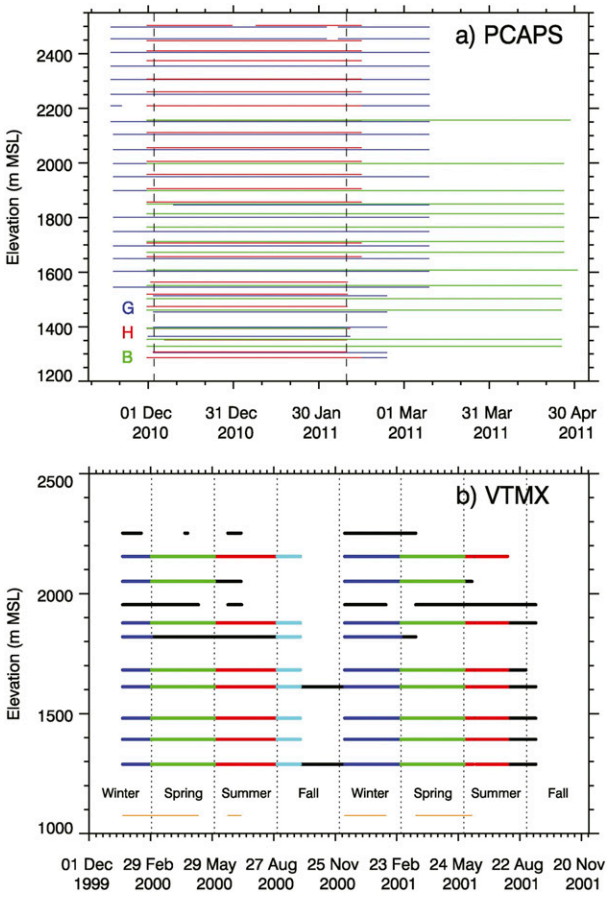

FIG. 2. Periods of record and missing data for the (a) PCAPS Grandeur (G, blue), Harker (H, red), and Bingham (B, green) and (b) VTMX HOBOs. Gaps indicate missing data. All available PCAPS and VTMX data are analyzed in section 3a. PCAPS data between the two vertical dashed lines in (a) and VTMX data for the combined subperiods indicated by the thin gold lines in (b) are analyzed in section 3b. In (b), subperiods going into the VTMX winter (blue), spring (green), summer (red), and fall (cyan) seasonal composites are indicated. VTMX seasonally composited data are analyzed in section 3c.

Because individual HOBOs had different periods of record and missing data points, the number of data pairs differs from HOBO to HOBO.

For the PCAPS soundings in winter and early spring, the mean 0415 MST PVT soundings are colder than the radiosonde soundings by 0°–2°C because of well-known shallow cold boundary layers or inversions that form on valley sidewalls (Zardi and Whiteman 2012). Temperature differences and standard deviations decrease above 1700 m MSL as the slopes steepen, the inversions above the steeper slopes become weaker and the slope atmosphere becomes better coupled to the ambient atmosphere.

With the exception of the Harker line, the mean 1615 MST PVT soundings are generally warmer than the radiosondes by 0°–2°C, with standard deviations between 0.8° and 1.8°C. The afternoon temperature excess is caused by the development of shallow slope-parallel warm boundary layers (Zardi and Whiteman 2012) and, to some extent, by the overheating of the radiation shields. The Harker line is colder than the radiosonde sounding, as it and the upper Bingham line fall into shadow before 1615 MST in midwinter. Because the Bingham line period of record extends into spring when it is again illuminated by the late afternoon sun, its mean temperature difference remains positive.

The VTMX PVT soundings are also colder than radiosonde soundings in the morning and warmer in the afternoon. This effect is stronger in the multiseason VTMX data than for the winter PCAPS data, and standard deviations are marginally higher, but generally still below 2°C. The exception is the much colder 0415 MST VTMX PVT profiles between the surface and 1700 m MSL; the difference reaches −4°C, with a standard deviation of 2.8°C at 1500 m MSL. The VTMX HOBO at 1490 m MSL is, however, affected by colder air that is channeled down a nearby shallow gully.

The colder nighttime and warmer daytime HOBO temperature differences tend to cancel when the 0415 and 1615 MST soundings are combined, so that the mean temperature differences fall in the range from −1.2° to 0.5°C, with standard deviations generally below 2°C except between the surface and 1800 m MSL where standard deviations reach 2°–3.5°C.

The uppermost HOBOs on both the PCAPS and VTMX lines are unusually cold relative to the radiosondes. This is most apparent in winter (and thus for the PCAPS lines) and is caused by the buildup in snow depth, which brings the HOBOs closer to the cold underlying snowpack and deeper into the near-surface temperature inversion. The uppermost sensors on the Grandeur line were extended above the snowpack occasionally as snow depth increased. None of the Bingham line HOBOs were buried, but the two uppermost sensors of the inaccessible Harker line showed a clear signal of being submerged in the snowpack. Data during these times are characterized by a sudden reduction in the amplitude of the diurnal temperature cycle. These data were excluded from the analysis.

b. Subsets, PCAPS and VTMX lines

Here, we analyze HOBO–radiosonde temperature differences for subsets of data during restricted time periods with no missing data. The same numbers of observations are then averaged at the different heights, the sensors are subject to the same large-scale weather systems, and PVT soundings are used to evaluate mean lapse rates. For the PCAPS period, the data subset runs

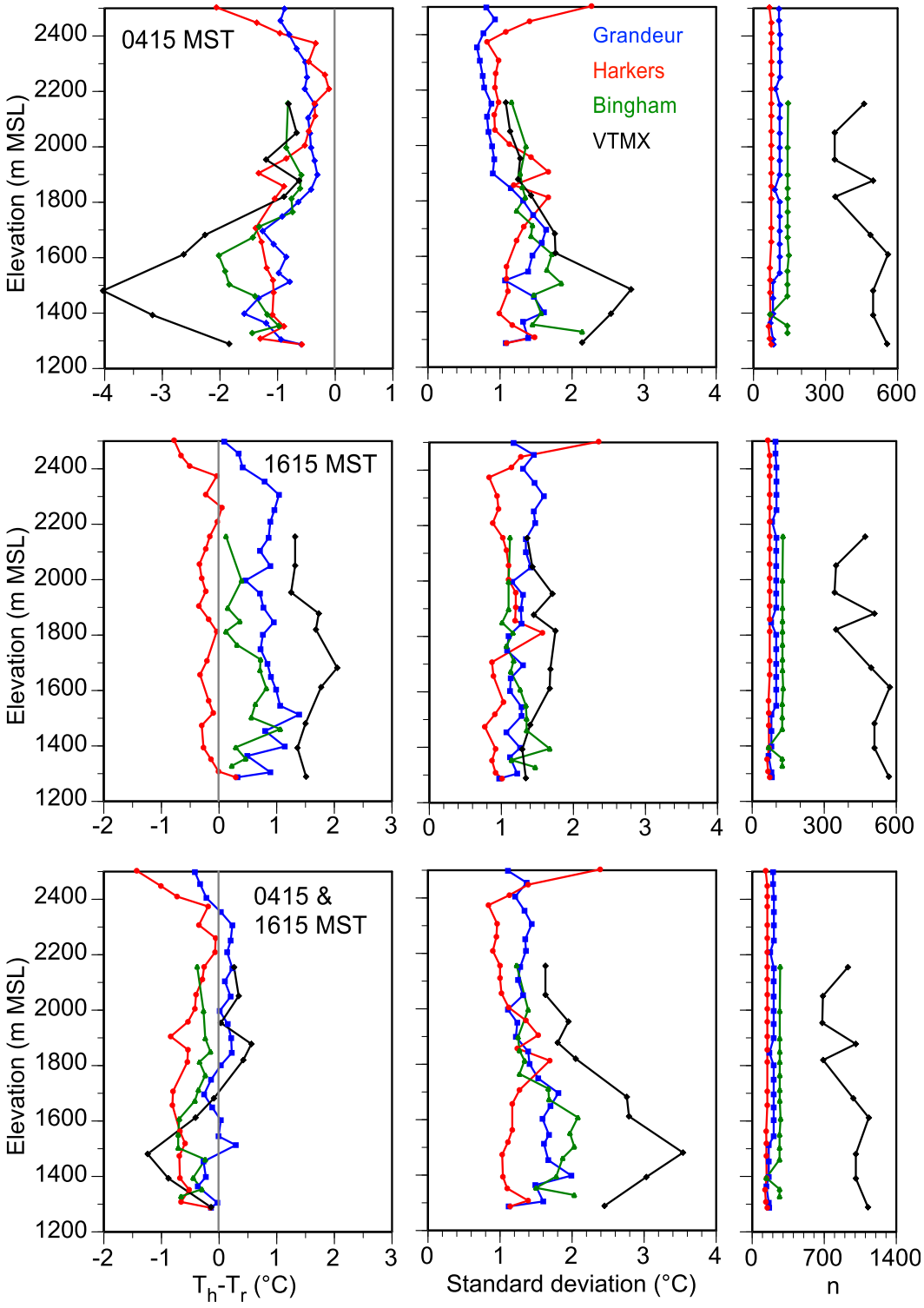

FIG. 3. HOBO–radiosonde mean temperature difference ($T_h - T_r$), standard deviation, and number of observations n for the Grandeur ridge, Harker ridge, Bingham, and VTMX lines for the (top) 0415 MST, (middle) 1615 MST, and (bottom) combined radiosonde sounding times.

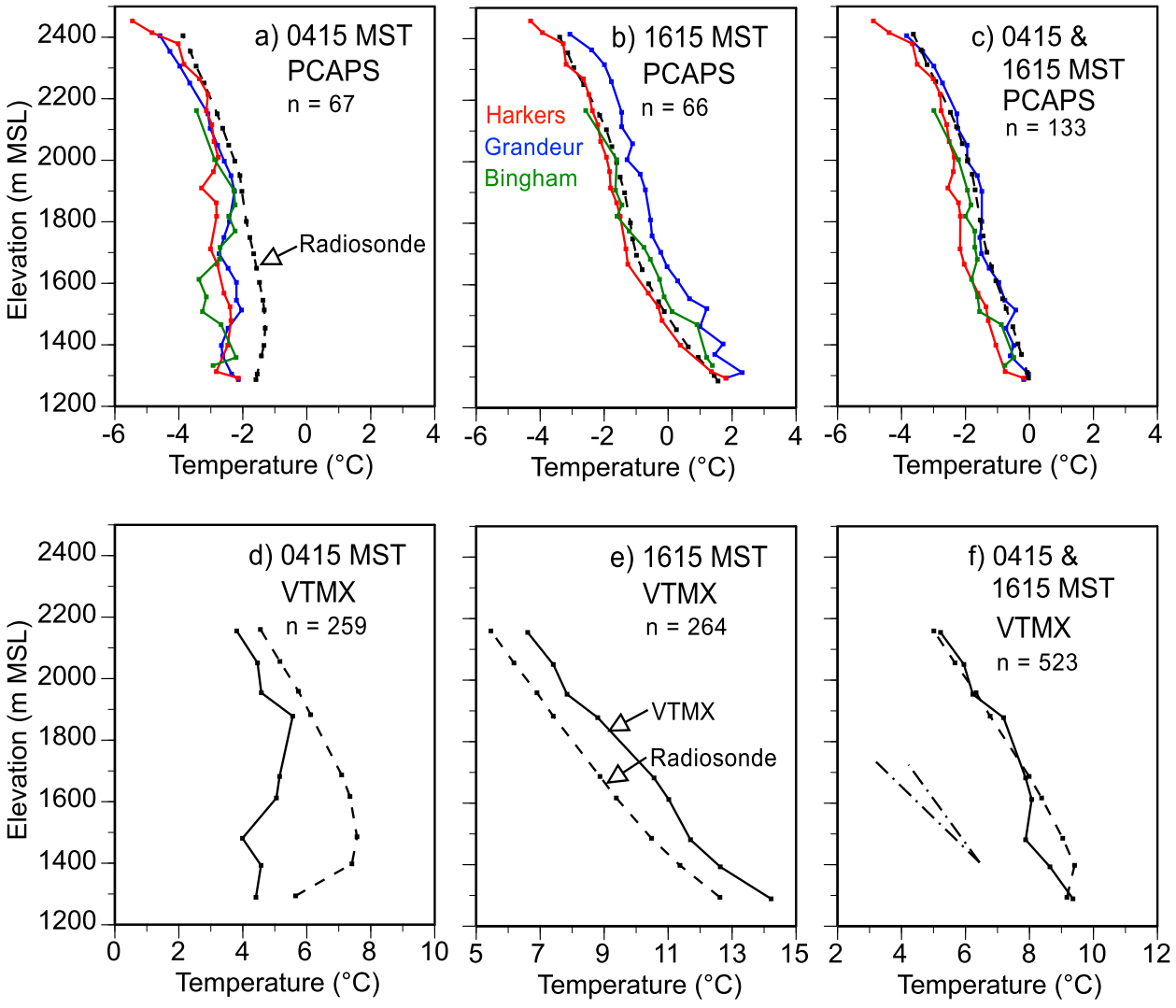

FIG. 4. Comparison of mean radiosonde temperature soundings (dashed lines) with mean pseudovertical HOBO sounding (solid lines) for restricted data periods from the (top) PCAPS and (bottom) VTMX lines at (a),(d) 0415 MST, (b),(e) 1615 MST, and (c),(f) both times. The number of observations n used to calculate the means is indicated. See Figs. 2a,b for the restricted periods of record for the PCAPS and VTMX data, respectively. The International Civil Aviation Organization (ICAO 1993) standard atmosphere (6.5°C km^{-1}) and dry-adiabatic (9.8°C km^{-1}) lapse rates (dashed–dotted lines) indicated in (f) can be compared with any of the subfigures, which all have the same aspect ratio.

from 2 December 2010 through 8 February 2011 (Fig. 2a). Figure 4 shows the mean temperature soundings for this period, and Table 1 provides vertically averaged mean PVT–radiosonde temperature differences.

The PCAPS 0415 MST mean PVT soundings for the three HOBO lines agree to within 0.5°C with the mean radiosonde sounding above 1800, 2000, and 1750 m, respectively. Below these heights, they are 1°–2°C colder than the radiosondes (Fig. 4a). While the Grandeur and Bingham lines show varying lapse rates, the Harker sounding parallels the radiosonde sounding. While the PVT soundings are near isothermal, a weak 200-m-deep inversion is present in the mean radiosonde sounding.

The PCAPS 1615 MST mean PVTs for the Bingham and Harker lines agree well with the radiosondes. Afternoon heating on the west-facing sidewall caused the Grandeur PVT sounding to be about 1°C warmer than the radiosonde (Fig. 4b). All PVT soundings match the vertically varying lapse rates well. The combined 0415 and 1615 MST mean PVT soundings agree with the radiosonde soundings within about 1°C and accurately match the lapse rates (Fig. 4c).

When comparing line-averaged differences (Table 1), the relative performance of the three PCAPS HOBO lines in replicating the radiosonde soundings varies between morning and afternoon. In the morning the

TABLE 1. Vertically averaged mean temperature differences between the HOBO and radiosonde soundings ($\Delta T = T_h - T_r$), the std dev of the mean temperature difference, and the number of HOBO–radiosonde comparisons n. These statistics are for restricted subsets of data bounded by the vertical dashed lines in Fig. 2a for the Grandeur, Harker, and Bingham lines, by the gold line segments in Fig. 2b for the "VTMX line all seasons," and by the green, red, cyan, and blue line segments in Fig. 2b for the VTMX spring, summer, fall, and winter seasons. Thus, the number of observations n is smaller than in Fig. 3.

HOBO lines	Time (MST)	ΔT (°C)	Std dev (°C)	n
Grandeur	0415	−0.67	1.14	67
	1615	0.72	1.24	66
	Both	0.02	1.40	133
Harker	0415	−0.79	1.15	67
	1615	−0.24	1.03	66
	Both	−0.51	1.14	133
Bingham	0415	−1.00	1.59	67
	1615	0.13	1.27	66
	Both	−0.44	1.58	133
VTMX line all seasons	0415	−1.67	1.66	259
	1615	1.35	1.47	264
	Both	−0.15	2.21	523
VTMX spring	0415	−1.87	1.73	171
	1615	1.77	1.17	179
	Both	−0.01	2.37	350
VTMX summer	0415	−2.87	2.05	138
	1615	2.26	1.40	136
	Both	−0.32	3.12	274
VTMX fall	0415	−2.47	1.53	31
	1615	1.97	1.41	31
	Both	−0.25	2.70	62
VTMX winter	0415	−1.16	1.46	116
	1615	0.48	1.19	120
	Both	−0.33	1.59	236

Grandeur ridge line is the best proxy for the free-air soundings, as near-surface temperature inversions are weaker on steep slopes than on low-angle slopes (Zardi and Whiteman 2012). Of the two HOBO lines on the west sidewall, the one closest to the sounding site (Harker) is next best and the farthest one (Bingham) is third. In the afternoon the best proxy is the Harker line, then the more distant Bingham line; the Grandeur line is a distant third, being warmed by late afternoon insolation.

The multiseasonal VTMX PVT soundings are poorer proxies for the radiosonde soundings than the wintertime PCAPS PVT soundings. Above 1800 m the mean 0415 MST PVT sounding parallels the radiosonde profile with an offset of less than 1.2°C. Below 1800 m, however, mean PVTs are up to 4°C colder, exhibiting a 1.5°C temperature inversion that extends to 1900 m MSL (Fig. 4d). The surface-based inversion in the radiosonde sounding is stronger (2°C) and extends only to 1500 m MSL.

The mean 1615 MST pseudovertical sounding parallels the radiosonde sounding but is 1°–1.5°C warmer (Fig. 4e). The combined 0415 and 1615 MST mean pseudovertical sounding agree closely with the mean radiosounding except between the surface and 1600 m MSL where the PVT sounding is from 0° to ~1°C colder (Fig. 4f).

c. *Seasonal effects, VTMX line*

The PCAPS wintertime PVT soundings are better proxies for free-air soundings than the all-season VTMX PVT soundings (see above). To investigate the seasonal variations in the PVT–radiosonde differences, we break the VTMX dataset into seasonally restricted time periods pieced together from subperiods in the period of record (see Fig. 2b) for which 9 of the 11 HOBOs had complete data.

Figure 5 presents the mean VTMX PVT and radiosonde soundings for each season at 0415 and 1615 MST, and for the combined 0415 and 1615 MST observations. Table 1 provides vertically averaged mean PVT–radiosonde temperature differences for the seasons. The PVT soundings are colder in the morning and warmer in the afternoon in all seasons, as expected, and have a much greater diurnal temperature range at all elevations than the radiosonde soundings, especially below 1900 m MSL. The winter, with its reduced insolation and high frequency of multiday cold-air pools, has a much lower diurnal temperature range than the other seasons. The greatest offsets between the PVT and radiosonde soundings are in summer, with the lowest offsets in spring.

Surface-based temperature inversions are present in the radiosonde soundings in all seasons at 0415 MST. Inversion strengths are 2.5°, 2.5°, 4°, and 1.5°C to heights of 1450, 1500, 1600, and 1450 m MSL in spring, summer, fall, and winter, respectively. In contrast, inversions extend to 1900 m MSL in the VTMX PVT soundings, with colder temperatures and weaker temperature gradients. Temperatures are considerably colder in the 1400–1600-m elevation range in the summer and fall.

Morning temperature deficits on the VTMX line indicate that there is spatial inhomogeneity in the valley, with additional cooling, more vertical mixing and deeper inversions in a subbasin in the southern part of the valley (Fig. 1) where cold air accumulates from the surrounding higher terrain. A cold-air layer along the slope (Whiteman and Zhong 2008) also contributes to the temperature deficit. A nighttime southerly low-level jet coming over the Traverse Range (Banta et al. 2004; Pinto et al. 2006) may provide the vertical shear and mixing that deepens the inversion. The north, open end of the valley at the radiosonde site is susceptible to intrusions; cold air drains out the valley exit there, producing shallower inversions.

Near-dry-adiabatic profiles are present through most of the valley depth in the 1615 MST radiosonde soundings above a near-surface superadiabatic layer. The

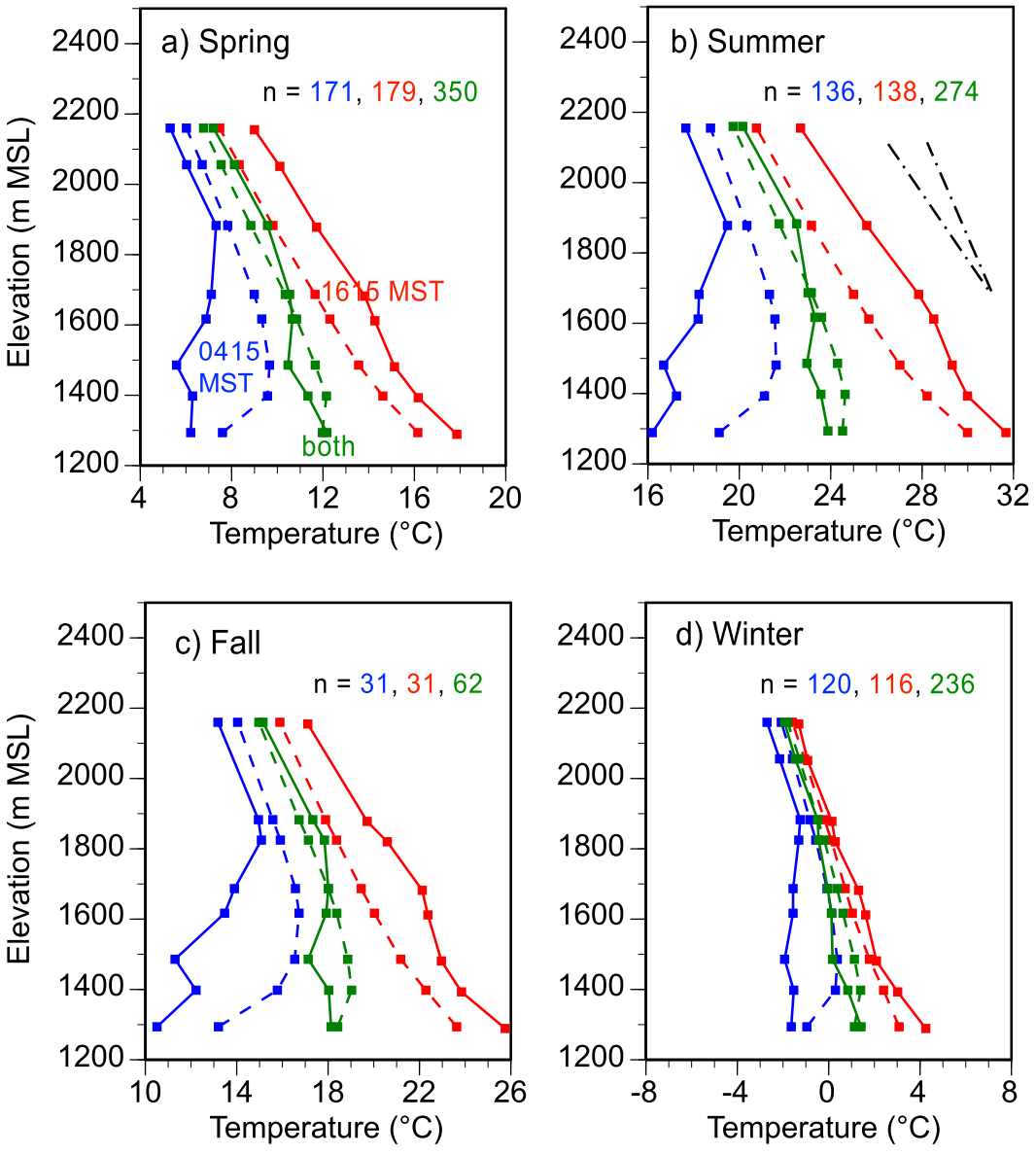

FIG. 5. (a) Spring, (b) summer, (c) fall, and (d) winter mean VTMX HOBO (solid lines) and radiosonde (dashed lines) soundings at 0415 MST (blue), 1615 MST (red), and both times combined (green). The number of pairs n of radiosonde and HOBO soundings used in computing the means is indicated. See Fig. 2b for the seasonal periods of record. The ICAO (1993) standard atmosphere (6.5°C km^{-1}) and dry-adiabatic (9.8°C km^{-1}) lapse rates (dashed–dotted lines) indicated in (b) can be compared with any of the subfigures, which all have the same aspect ratio.

pseudovertical soundings match the radiosonde temperature gradients quite well but are 1.5°–3°C warmer. Smaller offsets below 1550 m are probably related to higher soil moisture on the valley floor and thus greater latent heating. During the winter season, the PVT sounding prove to be the best proxy for the 1615 MST radiosonde, a time during which both insolation is at a minimum and the high albedo of snow cover reduces the sensible heating of the surface and thus the buildup of a strong superadiabatic layer.

The mean composited 0415 and 1615 MST radiosonde and VTMX soundings agree within 2°C through the whole valley depth, with the largest discrepancy at elevations of about 1500 m MSL.

4. Conclusions

Pseudovertical temperature soundings from lines of temperature sensors on the sidewalls of Utah's broad Salt Lake valley can provide a good proxy for radiosondes

launched twice per day at the north end of the valley. However, near-surface layers of cold air at night and warm air during daytime over the sidewalls result in significant offsets. Differences are largest near the valley floor where sidewalls are less steep, soil moisture is greater and cold-air pooling is enhanced. Agreement between PVT soundings and radiosondes increases with elevation, steepness of slope, and proximity to the radiosonde launch site. Nighttime and daytime lapse rates during PCAPS are best represented by the nearby Harker line, although larger offsets lead to larger total deviations. Lines of temperature sensors on the sidewalls of the broad Salt Lake valley provide valuable information on intravalley differences in meteorological phenomena.

Hitherto undocumented features of Salt Lake valley meteorology include the formation of cross-valley differences in temperature due to unequal insolation on the opposing sidewalls and the formation of deeper, colder inversions with weaker temperature gradients in the south part of the valley. These and other phenomena will be the focus of future work to gain additional knowledge of the meteorology of the valley. The 5-min PVT soundings provide much better time resolution than the radiosondes and would be operationally useful if data could be received in real time using newly available mesh networks of temperature sensors (e.g., Young et al. 2014).

Acknowledgments. National Science Foundation Grants ATM-0938397 (PCAPS) and AGS-1160730 (METCRAX II) and Kennecott Utah Copper Research Agreement 10020948 supported this research. We thank PCAPS and VTMX participants for their field support and the U.S. Department of Energy for VTMX research support.

REFERENCES

Banta, R. M., L. S. Darby, J. D. Fast, J. Pinto, C. D. Whiteman, W. J. Shaw, and B. D. Orr, 2004: Nocturnal low-level jet in a mountain basin complex. Part I: Evolution and effects on local flows. *J. Appl. Meteor.,* **43,** 1348–1365, doi:10.1175/JAM2142.1.

Clements, C. B., C. D. Whiteman, and J. D. Horel, 2003: Cold-air-pool structure and evolution in a mountain basin: Peter Sinks, Utah. *J. Appl. Meteor.,* **42,** 752–768, doi:10.1175/1520-0450(2003)042<0752:CSAEIA>2.0.CO;2.

Doran, J. C., J. D. Fast, and J. Horel, 2002: The VTMX 2000 campaign. *Bull. Amer. Meteor. Soc.,* **83,** 537–551, doi:10.1175/1520-0477(2002)083<0537:TVC>2.3.CO;2.

ICAO, 1993: *Manual of the ICAO Standard Atmosphere: Extended to 80 kilometres (262,500 feet).* 3rd ed. International Civil Aviation Organization, 304 pp.

Lareau, N., E. Crosman, C. D. Whiteman, J. D. Horel, S. W. Hoch, W. O. J. Brown, and T. W. Horst, 2013: The Persistent Cold-Air Pool Study. *Bull. Amer. Meteor. Soc.,* **94,** 51–63, doi:10.1175/BAMS-D-11-00255.1.

Lundquist, J. D., and D. R. Cayan, 2007: Surface temperature patterns in complex terrain: Daily variations and long-term change in the central Sierra Nevada, California. *J. Geophys. Res.,* **112,** D11124, doi:10.1029/2006JD007561.

——, N. Pepin, and C. Rochford, 2008: Automated algorithm for mapping regions of cold-air pooling in complex terrain. *J. Geophys. Res.,* **113,** D22107, doi:10.1029/2008JD009879.

Mayr, G. J., and Coauthors, 2004: Gap flow measurements during the Mesoscale Alpine Programme. *Meteor. Atmos. Phys.,* **86,** 99–119, doi:10.1007/s00703-003-0022-2.

Office of the Federal Coordinator for Meteorological Services and Supporting Research, 1997: Federal Meteorological Handbook No. 3: Rawinsonde and pibal observations. OFCM Doc. FCM-H3-1997, 191 pp. [Available online at www.ofcm.gov/fmh3/pdf/00-entire-FMH3.pdf.]

Pinto, J. O., D. B. Parsons, W. O. J. Brown, S. Cohn, N. Chamberlain, and B. Morley, 2006: Coevolution of down-valley flow and the nocturnal boundary layer in complex terrain. *J. Appl. Meteor. Climatol.,* **45,** 1429–1449, doi:10.1175/JAM2412.1.

Steinacker, R., and Coauthors, 2007: A sinkhole experiment in the Eastern Alps. *Bull. Amer. Meteor. Soc.,* **88,** 701–716, doi:10.1175/BAMS-88-5-701.

Whiteman, C. D., and S. Zhong, 2008: Downslope flows on a low-angle slope and their interactions with valley inversions. Part I: Observations. *J. Appl. Meteor. Climatol.,* **47,** 2023–2038, doi:10.1175/2007JAMC1669.1.

——, J. M. Hubbe, and W. J. Shaw, 2000: Evaluation of an inexpensive temperature datalogger for meteorological applications. *J. Atmos. Oceanic Technol.,* **17,** 77–81, doi:10.1175/1520-0426(2000)017<0077:EOAITD>2.0.CO;2.

——, S. Eisenbach, B. Pospichal, and R. Steinacker, 2004: Comparison of vertical soundings and sidewall air temperature measurements in a small Alpine basin. *J. Appl. Meteor.,* **43,** 1635–1647, doi:10.1175/JAM2168.1.

——, and Coauthors, 2008: METCRAX 2006: Meteorological experiments in Arizona's Meteor Crater. *Bull. Amer. Meteor. Soc.,* **89,** 1665–1680, doi:10.1175/2008BAMS2574.1.

——, S. W. Hoch, M. Lehner, and T. Haiden, 2010: Cold air intrusions into a closed basin: Observational evidence and conceptual model. *J. Appl. Meteor. Climatol.,* **49,** 1894–1905, doi:10.1175/2010JAMC2470.1.

Young, D. T., L. Chapman, C. L. Muller, and X.-M. Cai, 2014: A low-cost wireless temperature sensor: Evaluation for use in environmental monitoring applications. *J. Atmos. Oceanic Technol.,* **31,** 938–944, doi:10.1175/JTECH-D-13-00217.1.

Zardi, D., and C. D. Whiteman, 2012: Diurnal mountain wind systems. *Mountain Weather Research and Forecasting,* F. K. Chow, S. F. J. DeWekker, and B. Snyder, Eds., Springer, 35–119.

Zawar-Reza, P., M. Katurji, I. Soltanzadeh, T. Dallafior, S. Zhong, D. Steinhoff, B. Storey, and S. C. Cary, 2013: Pseudovertical temperature profiles give insight into winter evolution of the atmospheric boundary layer over the McMurdo Dry Valleys of Antarctica. *J. Appl. Meteor. Climatol.,* **52,** 1664–1669, doi:10.1175/JAMC-D-13-034.1.